Curr Cardiovasc Imaging Rep (2015) 8: 14
DOI 10.1007/s12410-015-9333-1

INTRAVASCULAR IMAGING (I.-K. JANG, SECTION EDITOR)

An Integrated Backscatter Ultrasound Technique for Coronary Plaque Imaging

Masanori Kawasaki

Published online: 5 March 2015
© Springer Science+Business Media New York 2015

Abstract The instability of atherosclerotic coronary plaques is related to their histological composition and the thickness of their fibrous caps. Therefore, recognition of the tissue characteristics of coronary plaques is important to understand and prevent coronary artery disease. Recently, an ultrasound integrated backscatter (IB) technique has been developed. Ultrasound signals have unique characteristics of reflection. That is, the ultrasound IB power ratio is a function of the difference in acoustic characteristic impedance between the medium and target tissue, and the acoustic characteristic impedance is determined by the density of tissue multiplied by the speed of sound. This principle allows for tissue characterization of coronary plaques for the risk stratification in patients with coronary artery disease. Two- and three-dimensional IB color-coded maps for the evaluation of tissue components can be constructed to detect four major components: fibrous, dense fibrosis, lipid pool, and calcification. Many studies have shown the reliability and usefulness of the IB technique.

Keywords Integrated backscatter · Ultrasound · Coronary artery · Plaque · Tissue · Imaging

Introduction

Tissue characteristics of coronary plaques have been reported to be associated with cardiovascular events [1, 2]. In 1966, Friedman et al. demonstrated that the communication between lumen and atheromatous abscess preceded and was responsible for the formation of the thrombus [3]. In 1978, Horie et al. examined serial sections of coronary arteries postmortem and demonstrated that plaque rupture into the vessel lumen sometimes preceded and caused thrombus formation, which resulted in acute myocardial infarction [4]. In 1992, Mizuno et al. demonstrated that disruption or erosion of vulnerable plaques followed by thrombosis was the most frequent cause of acute coronary syndrome (ACS) using a coronary angioscopy in vivo [5]. Therefore, tissue characterization of coronary plaques is important to evaluate the risk of cardiovascular disease.

Recently, an ultrasound integrated backscatter (IB) technique has been developed to analyze the tissue characteristics of coronary plaques. Recent in vivo studies demonstrated that ultrasound IB values reflected the tissue components of coronary atherosclerotic lesions. This article will summarize the ultrasound IB technique and its clinical usefulness for the stratification of risk for coronary artery diseases.

Concepts of the Ultrasound IB Technique and Methods for the Characterization of Coronary Tissue Components

The ultrasound IB power ratio is a function of the difference in acoustic characteristic impedance between the medium and target tissue, and the acoustic characteristic impedance is determined by the density of tissue multiplied by the speed of sound. The ultrasound IB power ratio is calculated using the following formula:

$$\text{Ultrasound IB power ratio} = 10\log\frac{(Z_2 - Z_1)^2}{(Z_2 + Z_1)^2}$$

This article is part of the Topical Collection on *Intravascular Imaging*

M. Kawasaki (✉)
Department of Cardiology, Gifu University Graduate School of Medicine, 1-1 Yanagido, Gifu 501-1194, Japan
e-mail: masanori@ya2.so-net.ne.jp

where Z_1 and Z_2 are the acoustic characteristic impedance of the medium and target tissue, respectively.

Therefore, as the difference in acoustic characteristic impedance between the medium and target is greater, the ultrasound IB power ratio becomes greater. With the IB ultrasound technique, ultrasound energy returns to the transducer after reflection from a small volume of tissue, and the IB values are calculated using a fast Fourier transform. The IB values are expressed as the average power, measured in decibels (dB).

With the use of commercially available transthoracic echocardiography, IB values can be automatically calculated from a region-of-interest (11×11 pixels, 0.6 mm×0.6 mm) set on an IB image (Sonos 5500 or 7500, Philips Medical Systems, Andover, MA, USA) [6]. In contrast, for the analysis of tissue characteristics using intravascular ultrasound (IVUS), a personal computer equipped with developed custom software was connected to an IVUS imaging system (VISIWAVE, Terumo, Tokyo, Japan) to obtain the ultrasound signal using a 38- and 43-MHz mechanically rotating IVUS catheter (ViewIT, Terumo, Tokyo, Japan) (Fig. 1) [7]. An analog-to-digital converter was used, which allowed acquisition of signals that were digitized at 400 MHz with 8-bit resolution. In the IVUS analysis, 512 vector lines of ultrasound signal around the circumference were analyzed to calculate the IB values. The IB values for each tissue component were calculated using a fast Fourier transform and expressed as the average power, measured in decibels, of the frequency component of the backscattered signal from a small volume of tissue. The tissue IB values were calibrated by subtracting the IB values from the IB value of a stainless steel needle placed at a distance of 1.5 mm from the catheter. IB-IVUS color-coded maps were constructed based on the IB values. Conventional IVUS images and IB-IVUS color-coded maps were immediately displayed side by side on a monitor (Fig. 2).

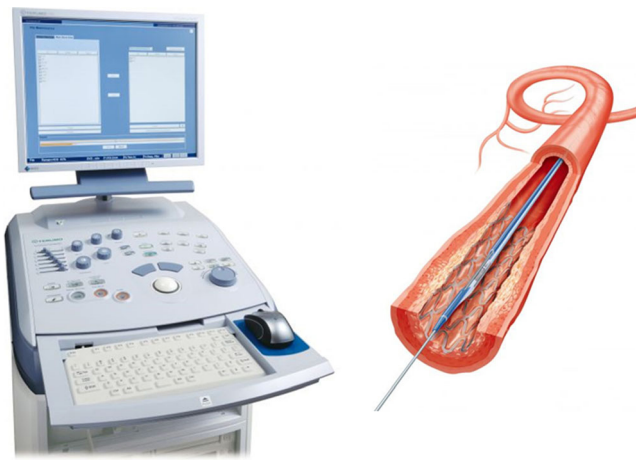

Fig. 1 Intravascular ultrasound system and intravascular ultrasound catheter

Diagnostic Accuracies of the Ultrasound IB Technique

With the IB-IVUS system, color-coded maps consist of four major components (fibrous [green], dense fibrosis [yellow], lipid pool [blue and purple], calcification [red]) (Fig. 3). The overall agreement between the classifications made by IB-IVUS and histology (lipid rich, fibrous, and fibrocalcific) was excellent (κ=0.83, 95 % CI 0.73–0.92) [8].

Comparison of the Thickness of Fibrous Cap Measured by IB-IVUS and Optical Coherence Tomography In Vivo

Recently, intravascular optical coherence tomography (OCT) was shown to provide high-resolution, cross-sectional images of plaques in situ with an axial resolution of 10 μm and a lateral resolution of 20 μm [9, 10]. According to a previous pathological and clinical review [11], thin fibrous cap with a large lipid core (thin-cap fibroatheroma) is one of the major criteria for vulnerable plaque that is prone to cause ACS. Therefore, measurement of the thickness of coronary plaques is important to evaluate the risk of cardiovascular disease.

To evaluate the accuracy of IB-IVUS for measurement of fibrous cap thickness, the same segments were compared by IB-IVUS and OCT (Fig. 4). The thickness of the fibrous cap measured by IB-IVUS was significantly correlated with that measured by OCT in the same coronary segments (Fig. 4) [7]. The mean difference between the thickness of fibrous cap measured by IB-IVUS and OCT was −2±147 μm (Fig. 5). OCT has a better potential for characterizing tissue components located in the near side from the vessel lumen, whereas IB-IVUS has a better potential for characterizing the tissue components of entire plaques.

Comparison with Virtual Histology Intravascular Ultrasound

Virtual Histology (VH) IVUS (Volcano Corporation, CA, USA) is one of the commercially available ultrasound techniques acquired with a 20-MHz phased-array catheter for tissue characterization of coronary plaques using an autoregressive classification scheme rather than depending on the classic Fourier method [12]. Hiro reported that VH-IVUS images are frequently patchy images of dense calcium and necrotic core [13••]. This is because VH-IVUS uses a classification tree with the eight values in order to discriminate necrotic core, fibro-fatty, fibrous, and dense calcium, and the classification tree branches for dense calcium and necrotic core are very close to each other.

For the qualitative comparison, the overall agreement between the histological and IB-IVUS diagnoses was higher (Cohen's κ=0.81, 95 % CI 0.74–0.90) than that between the histological and VH-IVUS diagnoses (Cohen's κ=0.30, 95 % CI 0.14–0.41) (Fig. 6) [8]. For the quantitative comparison, the % fibrosis area determined by IB-IVUS was significantly

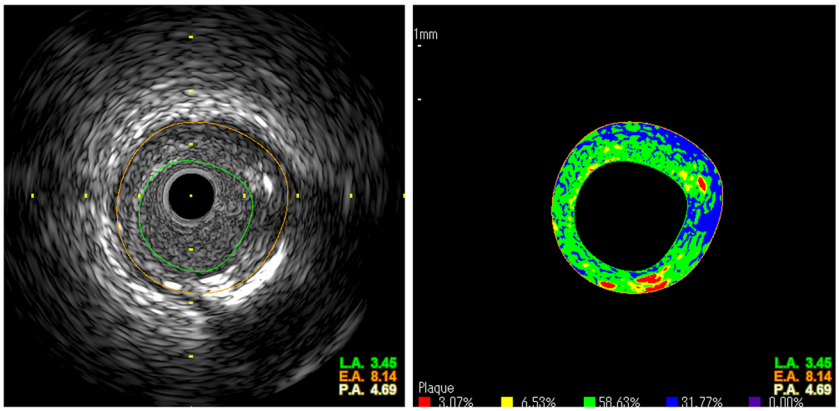

Fig. 2 A two-dimensional color-coded map of the coronary arterial plaque. Conventional IVUS images and IB-IVUS color-coded maps were displayed side by side on a monitor. Calculation of the relative area of each tissue characteristic was automatically performed by computer software. *Left*: conventional IVUS image. *Right*: two-dimensional color-coded map (*red*: calcification, *yellow*: dense fibrosis, *green*: fibrosis, *blue* and *purple*: lipid pool)

correlated with the relative area of fibrosis based on histology (r=0.67, p<0.001), whereas the % fibrous area and % fibrous area + % fibro-fatty area determined by VH-IVUS were not correlated with the relative area of fibrosis based on histology (Fig. 7) [8].

Application of Ultrasound IB Technique for the Evaluation of Plaques

Prediction of Adverse Events after Intervention Therapy Using IB Techniques

A prospective study was performed that determined the optimum cutoff value of relative lipid area in coronary segments without significant stenosis in patients who underwent percutaneous coronary intervention to predict future ACS [14].

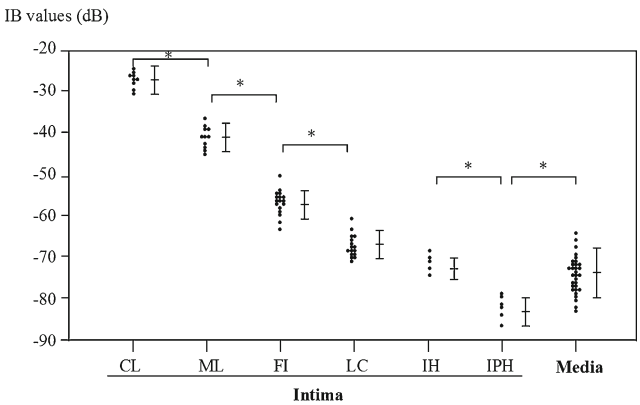

Fig. 3 Corrected IB values of various tissue types in coronary plaques. The corrected IB values from calcification (*CL*), mixed lesion (*ML*), fibrosis (*FI*), lipid pool (*LP*), intimal hyperplasia (*IH*), and intra-plaque hemorrhage (*IPH*) or media are significantly different from each other. However, there are no significant differences among lipid pool, intimal hyperplasia, and media. *Mixed lesion* is the region in which calcification and fibrosis were mixed. *p<0.05

Based on receiver-operating characteristic curve analysis, a relative lipid area of >65 % measured by IB-IVUS was found to be the optimal cutoff value for predicting ACS with a positive predictive value of 42 % and negative predictive value of 98 %. Lipid-rich plaques measured by IB-IVUS proved to be an independent morphologic predictor of non-target ischemic events after percutaneous coronary intervention, particularly in those patients with elevated serum C-reactive protein levels [15].

Glagov et al. demonstrated that positive remodeling in coronary plaques is a "compensatory process" to maintain the functional size of lumen as a safeguard against narrowing due to atherosclerotic progression with plaque accumulation [16]. Takeuchi et al. reported that relative lipid volume measured by IB-IVUS was greater in plaques with positive remodeling than plaques without positive remodeling, and they concluded that there were more lipid-rich components in lesions with positive remodeling than without positive remodeling, which may account for the higher incidence of ACS in those lesions with positive remodeling [17].

Uetani et al. reported that relative lipid volume (lipid volume/total plaque volume) measured by IB-IVUS correlated with post-procedural troponin-T and CK-MB levels that showed post-procedural myocardial injury after coronary stent implantation [18]. They concluded that a larger plaque volume and lipid-rich plaque were indicative of embolic events after stent implantation [18].

Effects of Statins on Atherosclerotic Plaques

HMG-Co-A reductase inhibitor drugs (statins) reduce the mortality of myocardial infarction and prevent the progression of atherosclerosis [19, 20]. Using three-dimensional IB-IVUS (Fig. 8), the effect of atorvastatin on coronary plaques was elucidated [21]. The relative lipid volume in coronary plaques measured by IB-IVUS significantly decreased in the statin

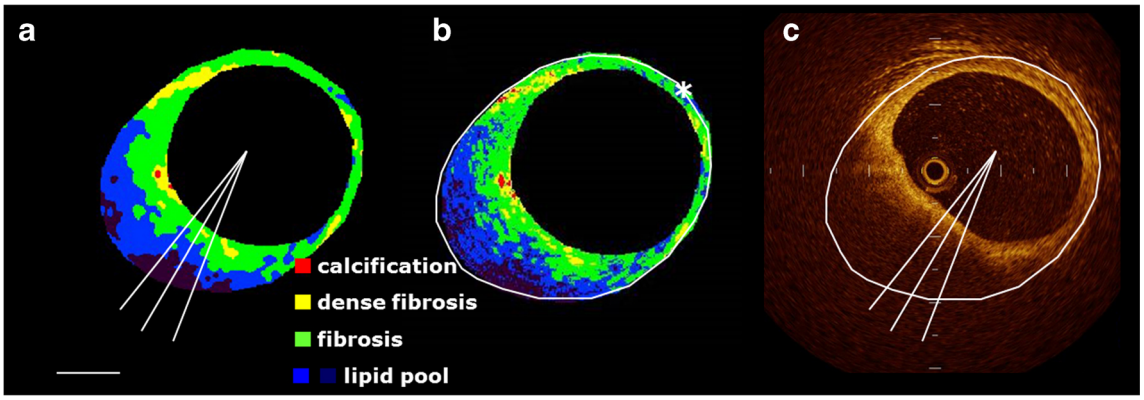

Fig. 4 **a** Representative integrated backscatter intravascular ultrasound (IB-IVUS) images processed by a smoothing method. **b** Original IB-IVUS images. **c** Corresponding optical coherence tomography images. *Bar*=1 mm

therapy group after 6 months, whereas lipid volume did not change significantly in the diet group. Otagiri et al. investigated the effectiveness of rosuvastatin in patients with ACS using IB-IVUS. They demonstrated that the magnitude of the reduction in relative lipid volume after 6 months of rosuvastatin was significantly correlated with the baseline value (r=−0.498, p=0.024) [22]. This regression was mainly due to a decrease in the lipid component measured by IB-IVUS. Early intervention with rosuvastatin in ACS patients resulted in a significant reduction of the non-culprit plaque after 6 months.

Comparison with Other Techniques

There are several ultrasound techniques for tissue characterization of coronary plaques [23]. iMap (Boston Scientific, MA, USA) is also one of the commercially available intravascular ultrasound systems for tissue characterization of coronary plaques. The iMap algorithm is based on a neural network theory especially for pattern recognition called the k-nearest neighbor method [24]. It measures a total of 40 values representing how the signal spectrum from the RF segment of interest is similar to each spectrum shape that is specific for necrotic, lipid, fibrotic, or calcified areas from the spectrum shape database library, which was previously obtained from cadaver hearts [24]. However, the number of reference points for lipid area is relatively small, and that area is frequently identified as smaller within a plaque than other types of tissue [25••]. Yamada et al. reported that necrotic tissue area by iMap correlated well with lipid pool area by IB-IVUS, whereas lipidic area by iMap did not correlate with lipid pool area by IB-IVUS, and tissue types classified by iMap generally correlated well with corresponding tissue type by IB-IVUS. However, there was some discrepancy between the two systems [25••].

Wavelet analysis is a mathematical model for the detection of lipid pools in coronary plaques reported by Murashige et al. [26]. The theoretical basis of wavelet analysis was first developed by Grossmann and Morlet [27]. Wavelet analysis is a time-frequency domain analysis of ultrasound signals. A wavelet is a short segmental waveform of limited duration that has an average value of zero. Wavelet patterns that meet various mathematical criteria have been proposed for comparison and results in many wavelet coefficients, C, which are a function of scale and position. The most appropriate C of wavelet coefficients for the detection of lipid pool

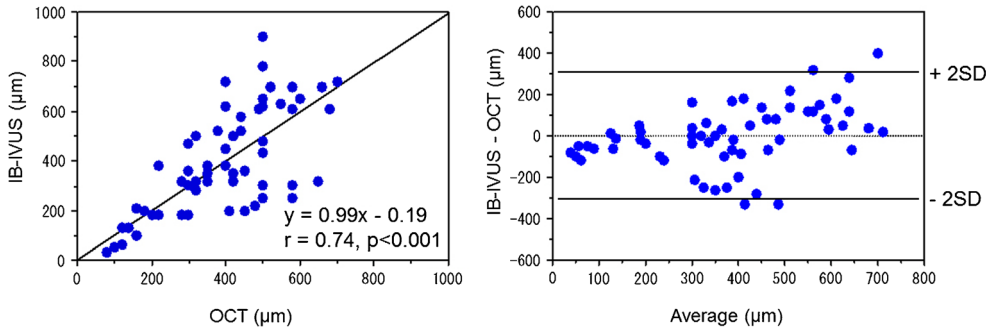

Fig. 5 *Left*: Correlation between the thickness of fibrous cap measured by integrated backscatter intravascular ultrasound and optical coherence tomography. *Right*: Bland-Altman plot

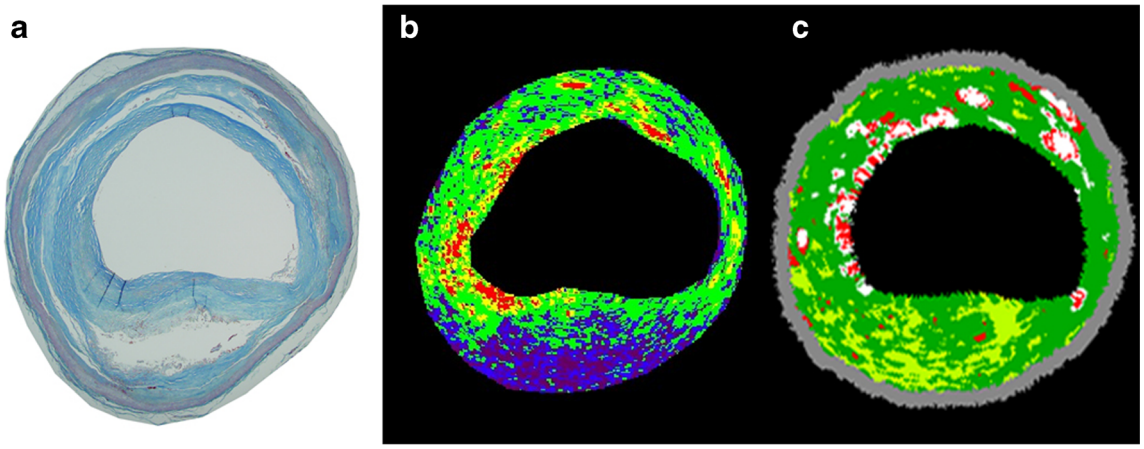

Fig. 6 **a** Representative IB-IVUS and VH-IVUS images at the same segment. **a** Histological image. **b** Corresponding IB-IVUS image. **c** Corresponding VH-IVUS image

was 0.6 with a sensitivity of 83 % and a specificity of 82 % [26]. The wavelet analysis is a unique and different method from IB-IVUS.

Recently, high-frequency ultrasound IVUS using 80 MHz without any particular mathematical processing has been proposed [28]. Compared to a 35-MHz ultrasonic image, the 80-MHz image showed superior resolution and contrast with imaging of a rabbit aorta in vivo. High-frequency IVUS is one of the promising methods for the tissue characterization of coronary plaques.

More recently, an integrated IVUS-OCT imaging apparatus, which includes the IVUS and OCT catheter, motor drive unit, and imaging system, has been developed [29]. An integrated IVUS-OCT imaging provides high-resolution and high-penetration depth for a better assessment of vulnerable plaques in in vivo animal studies [29]. After solving some potential technical issues, this integrated modality is promising for using in clinical studies.

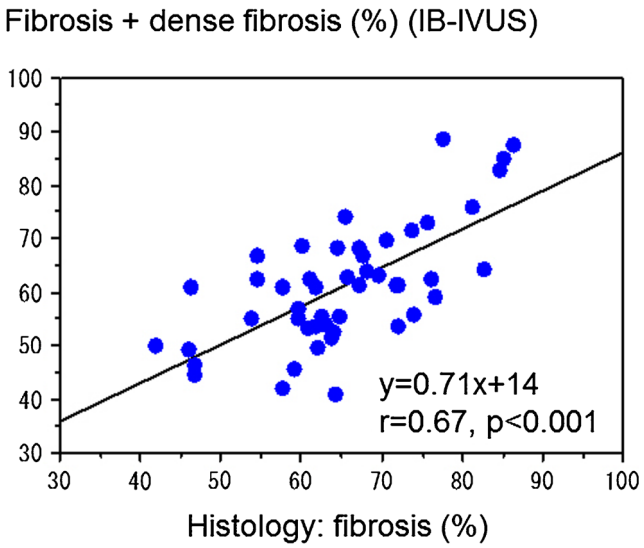

Fig. 7 Relationship between relative fibrous area measured by IB-IVUS and histology. Histological images that were stained with Masson's trichrome were digitized, and the areas that were stained blue were automatically selected by a multipurpose image processor (LUZEX F, Nireco Co., Tokyo, Japan). Then the relative fibrous area (fibrous area / plaque area) was automatically calculated by the LUZEX F system

Using IB-IVUS as a gold standard, a cutoff value of Hounsfield units (HU) for the differentiation between lipid pool and fibrosis was determined by comparing the same cross sections of coronary plaques depicted by IB-IVUS and multidetector row computed tomography (MDCT) [30••]. Using receiver-operating characteristic curve analysis, a threshold of 50 HU was the optimal cutoff value to discriminate lipid pool from fibrosis. As shown in Fig. 9, the distribution of tissue components based on 3D color-coded maps constructed from MDCT images was similar to the distribution based on 3D maps constructed from IB-IVUS images.

Technical Considerations of Ultrasound IB Techniques

Fixation and processing of vessels for histopathological examination has been reported to result in a decrease in total vessel cross-sectional area and luminal cross-sectional area, but absolute wall area (total vessel cross-sectional area minus luminal cross-sectional area) did not change in vessels with minimal atherosclerotic narrowing [31, 32]. Several studies have documented that formalin fixation does not significantly affect the morphology and quantitative echo characters of plaque tissue in the human aorta [6, 33].

IB-IVUS occasionally underestimates calcified lesions and overestimates lipid pool behind calcification due to the acoustic shadow derived from calcification. Acoustic shadow caused by calcification hinders precise

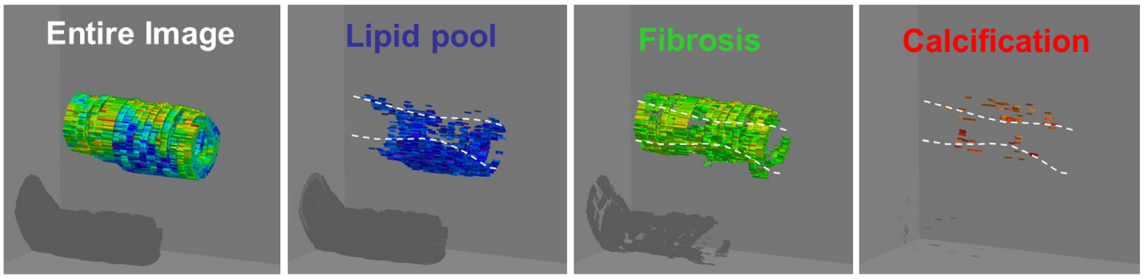

Fig. 8 Three-dimensional color-coded maps of the coronary arterial plaques constructed by IB-IVUS

determination of the tissue characteristics of coronary plaques. However, there have been many cases in which lesions that were classified as lipid pool by IB-IVUS due to the acoustic shadow behind calcification actually included lipid core in the same lesion analyzed by histology (n=16/21, 76 %) [34]. This finding was concordant with previous results demonstrating that necrotic core and fibro-fatty components were located behind calcification (83–89 %) [35]. Since calcification usually originates in lesions with lipid accumulation, the diagnosis of lipid pool by IB-IVUS in lesions behind calcification is usually accurate.

Limitations of the IB Technique

There were a few limitations of the ultrasound method. First, the angle dependence of the ultrasound signal makes tissue characterization unstable, when lesions are not perpendicular to the axis. Picano et al. reported that angular scattering behavior is large in calcified and fibrous tissues, whereas it is slight to non-existent in normal and fatty plaques [36]. According to that report, although there was no crossover of IB values between fibrous and fibro-fatty tissue within an angle span of 10°, or between fibrous and fatty tissue within an angle span of 14°, this angle dependence of the ultrasound signal might be partially responsible for the variation of IB values obtained from each tissue component. There was also a report that demonstrated the degree of angle dependence of 30-MHz ultrasound in detail [37]. In that report, the angle dependence of 30-MHz ultrasound in the arterial intima and media was 1.11 dB/10°. When a 40-MHz catheter was used, the angle dependence increased in arterial tissue. This angle dependence of the ultrasound signal may decrease the diagnostic accuracy for differentiating tissue components. Second, calcification is a perfect reflector for ultrasound, causing acoustic shadowing so typical in IVUS images. The ultrasound signals cannot penetrate or pass through the calcified layer and are reflected back towards the transducer [38]. Therefore, accurate tissue characterization of the areas behind calcification using IB-IVUS was not possible, as with conventional IVUS. Likewise, IB-IVUS cannot diagnose the tissue behind stents, because stents are nearly perfect reflectors causing acoustic shadowing of the ultrasound signal. This may also decrease the diagnostic accuracy for differentiating the tissue components. Third, a guidewire was not used in the process of imaging because the present studies were performed ex vivo. Imaging artifacts in vivo due to a guidewire may decrease diagnostic accuracy. Finally, detecting thrombus from a single IVUS cross section was not possible because we usually looked at multiple IVUS images over time for speckling, scintillation, motion, and blood flow in the

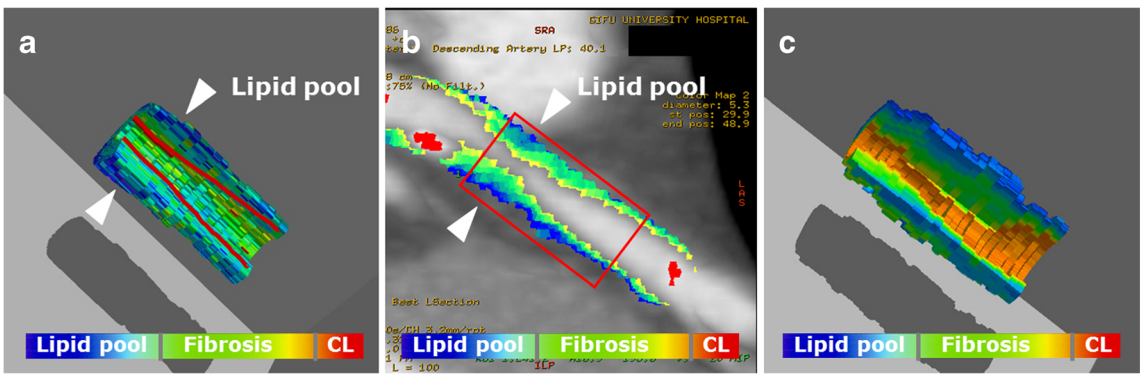

Fig. 9 Representative case of three-dimensional (3D) color-coded maps. 3D constructions were automatically performed by computer software. **a** 3D color-coded map of coronary plaque constructed by IB-IVUS. **b** Color-coded curved multiplanar reconstruction image of coronary plaque. **c** 3D color-coded map constructed by multidetector computed tomography for the same lesion as in **a**. *CL* calcification

"microchannel" [38]. The analysis of IB values in multiple cross sections over time is required for the detection of thrombus.

Conclusions

Ultrasound IB techniques that depend upon differences of acoustic characteristic impedance among various tissue components have been established for the tissue characterization of human coronary arteries. IB-IVUS can detect lipid pools and fibrous tissue in atherosclerotic lesions and can evaluate the effects of lipid-lowering therapy. Lipid-rich plaques are associated with the incidence of atherosclerotic diseases; therefore, ultrasound IB techniques can be useful to predict coronary artery diseases.

Compliance with Ethics Guidelines

Conflict of Interest Masanori Kawasaki declares that he has no conflict of interest.

Human and Animal Rights and Informed Consent This article does not contain any studies with human or animal subjects performed by any of the authors.

References

Papers of particular interest, published recently, have been highlighted as:
•• Of major importance

1. Virmani R, Kolodgie FD, Burke AP, et al. Lessons from sudden coronary death: a comprehensive morphological classification scheme for atherosclerotic lesions. Arterioscler Thromb Vasc Biol. 2000;20:1262–75.
2. Gronholdt ML, Nordestgaard BG, Schroeder TV, et al. Ultrasonic echolucent carotid plaques predict future strokes. Circulation. 2001;104:68–73.
3. Friedman M, Van den Bovenkamp GJ. The pathogenesis of a coronary thrombus. Am J Pathol. 1966;48:19–44.
4. Horie T, Sekiguchi M, Hirosawa K. Coronary thrombosis in pathogenesis of acute myocardial infarction. Histopathological study of coronary arteries in 108 necropsied cases using serial section. Br Heart J. 1978;40:153–61.
5. Mizuno K, Satomura K, Miyamoto A, et al. Angioscopic evaluation of coronary artery thrombi in acute coronary syndromes. N Engl J Med. 1992;326:287–91.
6. Kawasaki M, Takatsu H, Noda T, et al. Non-invasive tissue characterization of human atherosclerotic lesions in carotid and femoral arteries by ultrasound integrated backscatter: comparison between histology and integrated backscatter images before and after death. J Am Coll Cardiol. 2001;38:486–92.
7. Kawasaki M, Hattori A, Ishihara Y, et al. Tissue characterization of coronary plaques and assessment of thickness of fibrous cap using integrated backscatter intravascular ultrasound. Comparison with histology and optical coherence tomography. Circ J. 2010;74: 2641–8.
8. Okubo M, Kawasaki M, Ishihara Y, et al. Tissue characterization of coronary plaques: comparison of integrated backscatter intravascular ultrasound with virtual histology intravascular ultrasound. Circ J. 2008;72:1631–9.
9. Tearney GJ, Regar E, Akasaka T, et al. Consensus standards for acquisition, measurement, and reporting of intravascular optical coherence tomography studies: a report from the International Working Group for Intravascular Optical Coherence Tomography Standardization and Validation. International Working Group for Intravascular Optical Coherence Tomography (IWG-IVOCT). J Am Coll Cardiol. 2012;59:1058–72.
10. Jang IK, Tearney GJ, MacNeill B, et al. In vivo characterization of coronary atherosclerotic plaque by use of optical coherence tomography. Circulation. 2005;111:1551–5.
11. Naghavi M, Libby P, Falk E, et al. From vulnerable plaque to vulnerable patient: a call for new definitions and risk assessment strategies: part I. Circulation. 2003;108:1664–72.
12. Nair A, Kuban BD, Tuzcu EM, et al. Coronary plaque classification with intravascular ultrasound radiofrequency data analysis. Circulation. 2002;106:2200–6.
13.•• Hiro T. Three stars of the constellation of color intravascular ultrasound in the space of tissue characterization of coronary plaque. J Cardiol. 2013;61:186–7. *Important review of three commercially available systems for coronary tissue characterization*.
14. Sano K, Kawasaki M, Ishihara Y, et al. Assessment of vulnerable plaques causing acute coronary syndrome using integrated backscatter intravascular ultrasound. J Am Coll Cardiol. 2006;47:734–41.
15. Amano T, Matsubara T, Uetani T, et al. Lipid-rich plaques predict non-target-lesion ischemic events in patients undergoing percutaneous coronary intervention. Circ J. 2011;75:157–66.
16. Glagov S, Weisenberg E, Zarins CK, et al. Compensatory enlargement of human atherosclerotic coronary arteries. N Engl J Med. 1987;316:1371–5.
17. Takiuchi S, Rakugi H, Honda K, et al. Quantitative ultrasonic tissue characterization can identify high-risk atherosclerotic alteration in human carotid arteries. Circulation. 2000;102:766–70.
18. Uetani T, Amano T, Ando H, et al. The correlation between lipid volume in the target lesion, measured by integrated backscatter intravascular ultrasound, and post-procedural myocardial infarction in patients with elective stent implantation. Eur Heart J. 2008;29: 1714–20.
19. Taylor AJ, Kent SM, Flaherty PJ, et al. ARBITER: arterial biology for the investigation of the treatment effects of reducing cholesterol. A randomized trial comparing the effects of atorvastatin and pravastatin on carotid intima medial thickness. Circulation. 2002;106: 2055–60.
20. Long-Term Investigation with Pravastatin in Ischemic Disease (LIPID) Study Group: Prevention of cardiovascular events and death with pravastatin in patient with coronary heart disease and a broad range of initial cholesterol levels. N Engl J Med. 1998;339: 1349–57.
21. Kawasaki M, Sano K, Okubo M, et al. Volumetric quantitative analysis of tissue characteristics of coronary plaques after statin therapy using three dimensional integrated backscatter intravascular ultrasound. J Am Coll Cardiol. 2005;45:1946–53.
22. Otagiri K, Tsutsui H, Kumazaki S, et al. Early intervention with rosuvastatin decreases the lipid components of the plaque in acute coronary syndrome: analysis using integrated backscatter IVUS (ELAN study). Circ J. 2011;75:633–41.
23. Kawasaki M. An integrated backscatter ultrasound technique for the detection of coronary and carotid atherosclerotic lesions. Sensors. 2015;15:979–94.

24. Sathyanarayana S, Carlier S, Li W, et al. Characterisation of atherosclerotic plaque by spectral similarity of radiofrequency intravascular ultrasound signals. EuroIntervention. 2009;5:133–9.
25.•• Yamada R, Okura H, Kume T, et al. A comparison between 40 MHz intravascular ultrasound iMap imaging system and integrated backscatter intravascular ultrasound. J Cardiol. 2013;61:149–54. *Interesting comparison between IB-IVUS and iMAP.*
26. Murashige A, Hiro T, Fujii T, et al. Detection of lipid-laden atherosclerotic plaque by wavelet analysis of radio-frequency intravascular ultrasound signals: in vitro validation and preliminary in vivo application. J Am Coll Cardiol. 2005;45:1954–60.
27. Daubechies I, Grossmann A. An integral transform related to quantization. J Mat Phys. 1980;21:2080–90.
28. Li X, Wu W, Chung Y, et al. Novel PMN-PT free standing film for high frequency (80 MHz) intravascular ultrasonic imaging. IEEE Trans Ultrason Ferroelectr Freq Control. 2011;58:2281–8.
29. Li X, Li J, Jing J, et al. Integrated IVUS-OCT imaging for atherosclerotic plaque characterization. IEEE J Sel Top Quantum Electron. 2014;20:7100108.
30.•• Yamaki T, Kawasaki M, Jang IK, et al. Comparison between integrated backscatter intravascular ultrasound and 64-slice multi-detector row computed tomography for tissue characterization and volumetric assessment of coronary plaques. Cardiovasc Ultrasound. 2012;10:33. *Interesting comparison between IB-IVUS and multi-detector row computed tomography.*
31. Lockwood GR, Ryan LK, Hunt JW, et al. Measurement of the ultrasound properties of vascular tissue and blood from 35-65 Mhz. Ultrasound Med Biol. 1991;17:653–66.
32. Siegel RJ, Swan K, Edwalds G, et al. Limitations of postmorterm assessment of human coronary artery size and luminal narrowing: differential effects of tissue fixation and processing on vessel with different degrees of atherosclerosis. J Am Coll Cardiol. 1985;5:342–6.
33. Picano E, Landini L, Distante A, et al. Different degreed of atherosclerosis detected by backscattered ultrasound: an in vitro study on fixed human aortic walls. J Clin Ultrasound. 1983;11:375–9.
34. Okubo M, Kawasaki M, Ishihara Y, et al. Development of integrated backscatter intravascular ultrasound for tissue characterization of coronary plaques. Ultrasound Med Biol. 2008;34:655–63.
35. Kume T, Okura H, Kawamoto T, et al. Assessment of the histological characteristics of coronary arterial plaque with severe calcification. Circ J. 2007;71:643–7.
36. Picano E, Landini L, Distante A, et al. Angle dependence of ultrasonic backscatter in arterial tissues: a study in vitro. Circulation. 1985;72:572–6.
37. Courtney BK, Robertson AL, Maehara A, et al. Effect of transducer position on backscattered intensity in coronary arteries. Ultrasound Med Biol. 2002;28:81–91.
38. Mintz GS, Nissen SE, Anderson WD, et al. American College of Cardiology clinical expert consensus document on standards for acquisition, measurement and reporting of intravascular ultrasound studies (IVUS). A report of the American College of Cardiology task force on clinical expert consensus documents developed in collaboration with the European Society of Cardiology endorsed by the Society of Cardiac Angiography and Interventions. J Am Coll Cardiol. 2001;37:1478–92.